Vertical and radial motions in a tropical cyclone

By MARIANO A. ESTOQUE, *University of Hawaii*[1]

(Manuscript received June 19, 1962)

ABSTRACT

The vertical and radial motions associated with a given tangential velocity and temperature distribution corresponding to a tropical cyclone are calculated using a diagnostic equation. The equation is derived by introducing the hydrostatic and gradient wind approximations systematically into the meteorological equations. The computed circulation pattern appears to reproduce most of the important characteristics of a mature cyclone such as the eye and the eyewall. The results also show that the sinking motion in the eye is thermally controlled.

1. Introduction

The velocity field in a fully developed tropical cyclone exhibits a high degree of symmetry with respect to its axis of rotation. Its tangential component is in approximate gradient balance for considerable periods of time in spite of the disturbing influences of friction and non-adiabatic heating. It is, therefore, logical to expect that an appropriate distribution of the vertical and radial velocities are maintaining this quasi-balanced state. One may, in fact, derive an expression relating the radial and vertical circulations with given tangential wind and temperature distributions using an approach described by ELIASSEN (1952, 1959). Such an expression has been derived and integrated. This paper describes the results of the calculations.

2. The Model Equations

The basic assumptions which are made are as follows:

a. axial symmetry and hydrostatic equilibrium
b. gradient wind balance along the radial direction
c. neglect of local density change in the continuity equation.

Using these assumptions, one may write the basic meteorological equations in cylindrical coordinates as

$$\frac{\partial u}{\partial t}+v\frac{\partial u}{\partial r}+w\frac{\partial u}{\partial z}+v\left(f+\frac{u}{r}\right)=\frac{\partial}{\partial z}\left(K\frac{\partial u}{\partial z}\right)+\frac{\partial}{\partial r}\left[K_H\left(\frac{\partial u}{\partial r}+\frac{u}{r}\right)\right] \tag{1}$$

$$u\left(f+\frac{u}{r}\right)=\theta_s\frac{\partial \phi^*}{\partial r} \tag{2}$$

$$\frac{\partial \phi^*}{\partial z}=-\frac{g}{\theta} \tag{3}$$

$$\frac{\partial}{\partial r}(r\varrho_s v)+\frac{\partial}{\partial z}(r\varrho_s w)=0 \tag{4}$$

$$\frac{\partial \theta}{\partial t}+v\frac{\partial \theta}{\partial r}+w\frac{\partial \theta}{\partial z}=\frac{\partial}{\partial z}\left(K\frac{\partial \theta}{\partial z}\right)+K_H\left(\frac{\partial^2\theta}{\partial r^2}+\frac{1}{r}\frac{\partial \theta}{\partial r}\right)+\Gamma^* w \tag{5}$$

where
$$\phi^*\equiv C_p\left(\frac{p}{p_0}\right)^{R/C_p}$$

$$\Gamma^*\equiv\begin{cases}0, & w\leqslant 0\\ \dfrac{L}{\phi^*}\dfrac{\partial q_m}{\partial z}, & w>0\end{cases}$$

The subscript "s" on θ and ϱ indicate values for a standard tropical atmosphere; q_m is the saturated mixing ratio corresponding also to a standard atmosphere. Equations (1), (2), and

[1] Contribution No. 40, Hawaii Institute of Geophysics.

(3) represent the equations of motion along the tangential, radial, and vertical directions on the basis of assumptions (a) to (b). Equations (4) is the equation of continuity while (5) is the thermodynamic energy equation. According to the Eq. (5), heat is released by condensation wherever the motions are upward; no evaporational cooling occurs for downward motions. It may be seen that Eqs. (1) to (5) form a complete set with u, v, w, p, and θ as unknowns which may be used to study the evolution of an initially prescribed atmospheric condition. It may be shown also that only the distributions of u and θ need to be prescribed to start the solution.

We will now proceed to obtain a relationship between the motions (v and w) on the $r-z$ plane and the specified u and θ distributions. This is an essential step in the solution of the initial value problem because it will enable us to solve for the initial distributions of v and w which are necessary in computing the radial and vertical advections of u and θ in Eqs. (1) and (5). Eliminating ϕ^* from Eqs. (2) and (3) by cross differentiation, one obtains the thermal wind relationship

$$\left(f+\frac{2u}{r}\right)\frac{\partial u}{\partial z}=\frac{g\theta_s}{\theta^2}\frac{\partial\theta}{\partial r}+\frac{u}{\theta_s}\left(f+\frac{u}{r}\right)\frac{\partial\theta_s}{\partial z}$$

This equation is then differentiated with respect to time and the terms, $\partial u/\partial t$ and $\partial\theta/\partial t$, are eliminated by using Eqs. (1) and (5). The resulting equation will involve both v and w. If combined with Eq. (4) with the aid of the Stokes stream function, ψ, the equation reduces to

$$A\frac{\partial^2\psi}{\partial r^2}+B\frac{\partial^2\psi}{\partial r\partial z}+C\frac{\partial^2\psi}{\partial z^2}+D\frac{\partial\psi}{\partial r}+E\frac{\partial\psi}{\partial z}+H=0 \qquad (6)$$

where $$\frac{\partial\psi}{\partial z}=\varrho_s rv;\ \frac{\partial\psi}{\partial r}=\varrho_s rw$$

and

$$A=\frac{g\theta_s}{\theta^2}\frac{\partial\theta}{\partial z}$$

$$B=-\left(f+\frac{2u}{r}\right)\frac{\partial u}{\partial z}-\frac{g\theta_s}{\theta^2}\frac{\partial\theta}{\partial r}$$

$$C=\left(f+\frac{2u}{r}\right)\left(\frac{\partial u}{\partial r}+f+\frac{u}{r}\right)$$

$$D=-\left[\frac{2}{r}\frac{\partial u}{\partial z}-\frac{\left(f+\frac{2u}{r}\right)}{\theta_s}\frac{\partial\theta_s}{\partial z}\right]\frac{\partial u}{\partial z}-\left(f+\frac{2u}{r}\right)\cdot\left(\frac{\partial^2 u}{\partial z^2}-\frac{1}{\varrho_s}\frac{\partial\varrho_s}{\partial z}\frac{\partial u}{\partial z}\right)-\frac{2g\theta_s}{\theta^3}\frac{\partial\theta}{\partial r}\frac{\partial\theta}{\partial z}+\frac{g\theta_s}{\theta^2}\cdot\left(\frac{\partial^2\theta}{\partial r\partial z}-\frac{1}{r}\frac{\partial\theta}{\partial z}\right)$$

$$E=\left(\frac{2}{r}\frac{\partial u}{\partial z}-\frac{f+\frac{2u}{r}}{\theta_s}\frac{\partial\theta_s}{\partial z}\right)\left(f+\frac{u}{r}+\frac{\partial u}{\partial r}\right)-\left(f+\frac{2u}{r}\right)\cdot\left[\frac{1}{\varrho_s}\frac{\partial\varrho_s}{\partial z}\left(f+\frac{u}{r}+\frac{\partial u}{\partial r}\right)-\frac{1}{r}\frac{\partial u}{\partial z}-\frac{\partial^2 u}{\partial r\partial z}\right]+\frac{2g\theta_s}{\theta^3}\left(\frac{\partial\theta}{\partial r}\right)^2+\frac{g\theta_s}{\theta^2}\left(\frac{1}{r}\frac{\partial\theta}{\partial r}-\frac{\partial^2\theta}{\partial r^2}\right)$$

$$H=\left[\left(\frac{2}{r}\frac{\partial u}{\partial z}-\frac{\left(f+\frac{2u}{r}\right)}{\theta_s}\frac{\partial\theta_s}{\partial z}\right)F+\left(f+\frac{2u}{r}\right)\frac{\partial F}{\partial z}+\frac{2g\theta_s}{\theta^3}\frac{\partial\theta}{\partial r}F'-\frac{g\theta_s}{\theta^2}\frac{\partial F'}{\partial r}\right]\varrho_s r$$

$$F=\frac{\partial}{\partial z}\left(K\frac{\partial u}{\partial z}\right)+\frac{\partial}{\partial r}\left[K_H\left(\frac{\partial u}{\partial r}+\frac{u}{r}\right)\right]$$

$$F'=\frac{\partial}{\partial z}\left(K\frac{\partial\theta}{\partial z}\right)+K_H\left(\frac{\partial^2\theta}{\partial r^2}+\frac{1}{r}\frac{\partial\theta}{\partial r}\right)+\Gamma^* w$$

This equation enables one to solve for the stream function and, hence, v and w, in terms of the frictional and nonadiabatic forcing function, H.

It will be noted that the heat released by condensation, which is properly a function of ψ through w, is treated as part of the forcing function. This artifice is necessary in order to avoid difficulties in obtaining solutions by insuring the ellipticity of the differential equation for customarily observed u and θ distributions. The dependence of condensation on vertical motion will be approximated by an iterative procedure described by ELIASSEN (1959) and PEDERSEN (1961).

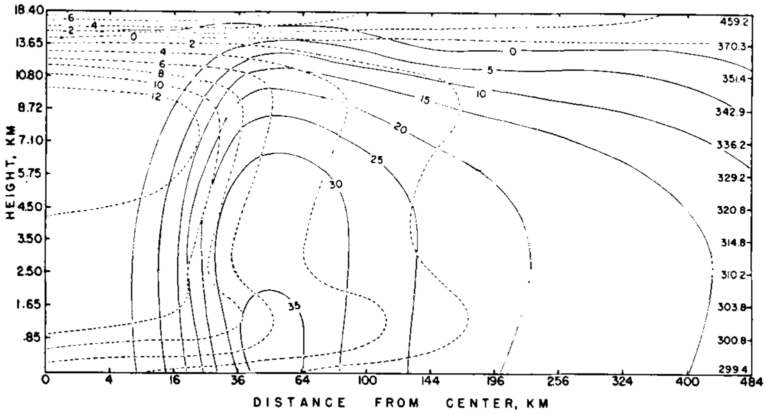

FIG. 1. The given tangential wind speed (m sec^{-1}) and potential temperature anomaly (°A) distributions. The anomaly is based on the average values shown on the right hand side.

3. Numerical Solution

The distribution of the stream function, ψ, was obtained by solving Eq. (6) with the given potential temperature and tangential wind distributions shown in Fig. 1. These distributions have been drawn on the basis of mean hurricane data. The bottom of the grid represents standard anemometer level while the left lateral boundary coincides with the axis of the storm. The two other boundaries have been chosen to be sufficiently distant so that the disturbance may be assume to be negligible at these boundaries. The stream function has been prescribed to be constant (zero) along the boundaries. In addition, we have assume certain boundary conditions for computing the forcing function, H. These are

At the bottom ($z=0$): $K\dfrac{\partial u}{\partial z}=\gamma u^2$

At the top ($z=18.40$ km): $K\dfrac{\partial u}{\partial z}=0$

At the lateral boundaries ($r=0$, $r=484$ km):

$$\frac{\partial}{\partial z}\left(K\frac{\partial \theta}{\partial z}\right)=K_H\frac{\partial^2\theta}{\partial r^2}=\frac{K_H}{r}\frac{\partial\theta}{\partial r}=0$$

where γ is the drag coefficient. The last condition implies no turbulent heat exchange effects at the lateral boundaries.

Using these boundary conditions in conjunction with a rectangular grid system, we computed the coefficients, A to E, and the forcing function, H, at every grid point. These quantities were then used together with a finite difference analog of Eq. (6) to solve for the stream function by relaxation.

Folllowing ELIASSEN (1959), the first relaxation was made without including the effect of heating by condensation. This gave a first estimate, ψ_0, of the stream function which is that resulting only from the turbulent mixing terms in the forcing function. The release of heat by condensation due to ψ_0 implies an increment, ΔH, in the forcing function. This increment is then used as a new forcing function to obtain the corresponding increment, $\Delta\psi_1$, in the stream function. The heating due to $\Delta\psi_1$ again gives an increment in the forcing function and, therefore, another increment, $\Delta\psi_2$, in the stream function and so forth. The total stream function due to both turbulent mixing and condensation heating is the sum

$$\psi=\psi_0+\Delta\psi_1+\Delta\psi_2+\ldots=\psi_0+\frac{\Delta\psi_1}{1-k}$$

For a temperature distribution which is near moist adiabatic, Eliassen has suggested a value of k equal to 0.5.

The first computation was made on a 12×12 grid with variable spacing in both radial and vertical directions as indicated in Fig. 1. This was necessary due to the limited capacity of the available computer. The variable spacing along the radial direction turned out to be unsatisfactory near $r=0$. Here, the horizontal gradients of the different variables were large and the grid spacing, relatively uneven. In

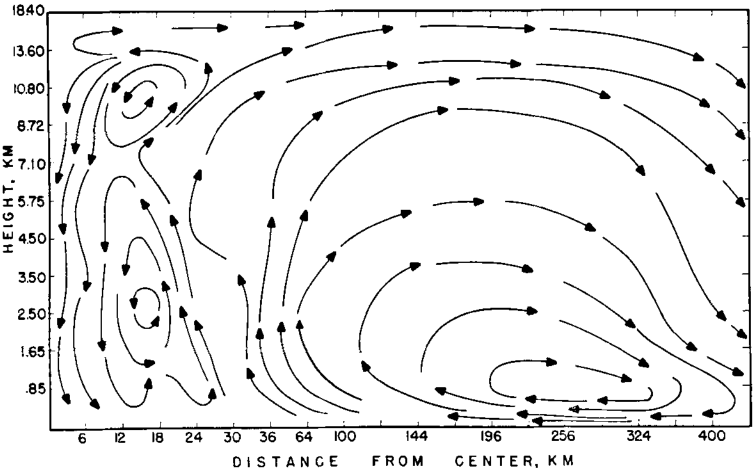

FIG. 2. The computed flow pattern. The lines indicate only direction of flow but not speed.

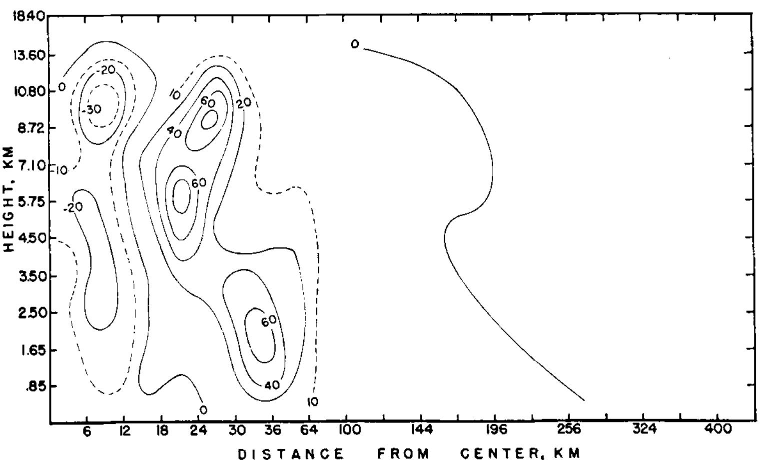

FIG. 3. The vertical velocity field in cm sec^{-1}.

order to eliminate this source of error, we made another computation using an equally-spaced grid of 6 km interval in the region $r = 0$ to $r = 66$ km. The relaxation for the stream function in this region used the results of the first computation as boundary values at $r = 66$ km.

The vertical exchange coefficient was assumed to decrease linearly with height with a value equal to 10^5 cm^2 sec^{-1} at the bottom and zero at the top. The lateral exhange coefficient and the drag coefficient were held constant with values of 10^9 cm^2 sec^{-1} and 2.5×10^{-3}, respectively; these appear to be reasonably close to the magnitudes indicated in a recent study by RIEHL and MALKUS (1961).

4. Results

The general characteristics of the computed radial and vertical motion fields are shown in Figs. 2 to 9. In Fig. 2, the arrow shafts are drawn parallel to the isolines of the stream function but are not spaced according to the computed speed; they may be considered, therefore, as stream lines on a vertical plane. On the whole, there is a striking resemblance between the computed circulation and that which is generally accepted for a mature storm. There is a region of downward motions in the central area (Fig. 3) which extends out to a radius of 15 km. The sinking motion is strongest near the

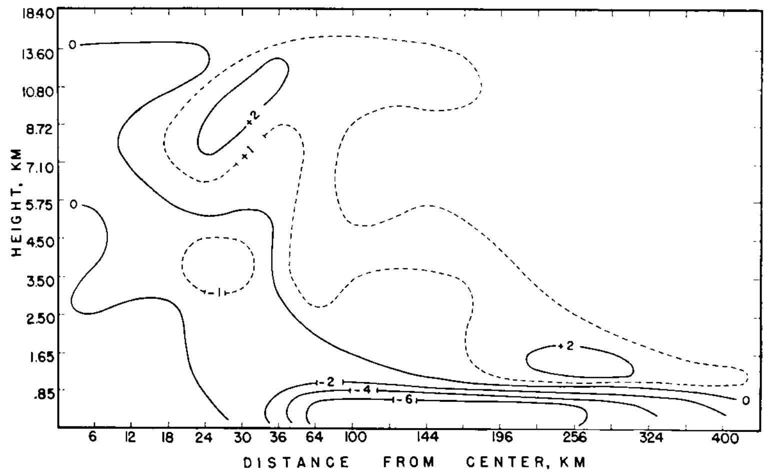

FIG. 4. The radial velocity field in m sec^{-1}.

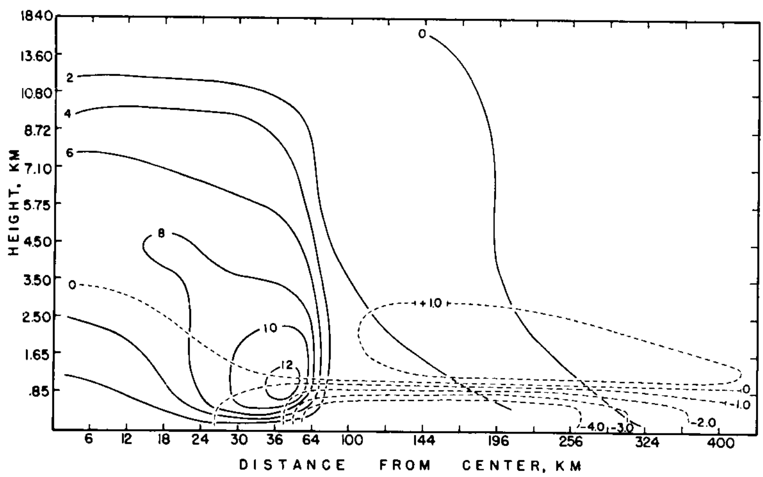

FIG. 5. The contributions to the vertical (cm sec^{-1}, full lines) and the radial (m sec^{-1}, dashed lines) velocity fields by vertical eddy diffusion of the tangential wind component.

10-km level with a maximum of about 30 cm sec^{-1}. Surrounding this eye is a ring of ascending motions which are very strong (80 cm sec^{-1}) at a distance of approximately 20 to 30 km from the center and slightly inward with respect to the zone of maximum winds. Although this general location appears to be reasonable, it does not agree completely with some evidence (Lavoie, 1956) indicating that the strongest upward motions are located in the zone of maximum winds. The outer region ($r > 200$ km) is characterized by very slow descending motions. Here, the computations indicated maximum values of about 2 cm sec^{-1} near an altitude of 1 km.

The radial wind distribution shows a relatively shallow layer of inflow adjoining the bottom and outflow near the top. The thickness of the inflow which is about 1 km at large distances from the center, gradually increases as the eye is approached. The magnitude of the radial inflow attains a maximum of almost 7 m sec^{-1} just below the 1 km level over a wide zone between $r = 100$ km and $r = 200$ km. In the lowest layers of the central core, there is a weak radial outflow.

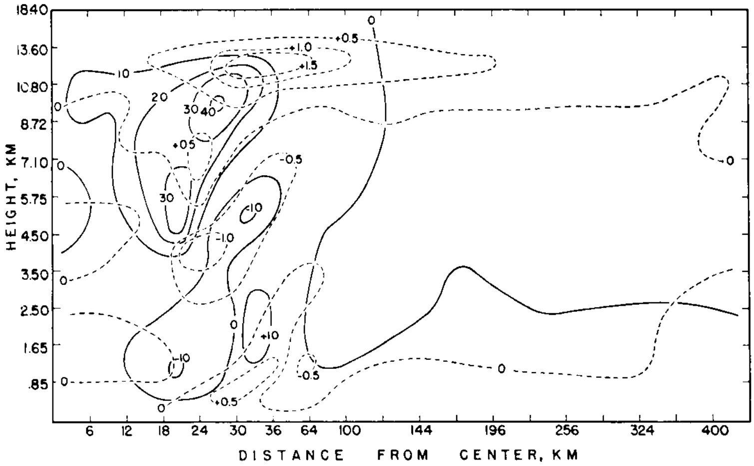

FIG. 6. The contributions to the vertical (cm sec^{-1}, full lines) and the radial (m sec^{-1}, dashed lines) velocity fields by lateral eddy diffusion of the tangential wind component.

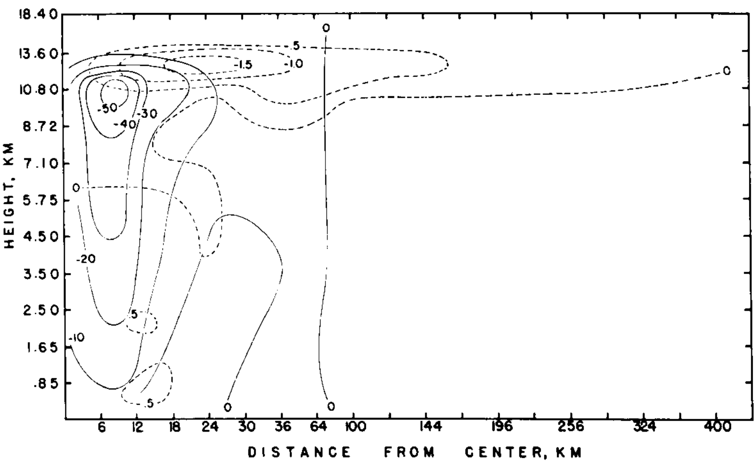

FIG. 7. The contributions to the vertical (cm sec^{-1}, full lines) and the radial (m sec^{-1}, dashed lines) velocity fields by lateral eddy diffusion of heat.

At this juncture, it is interesting to determine the relative importance of the various processes which contribute to the vertical circulation. In accordance with Equation (6), these may be considered as the following:

a. vertical eddy diffusion of the tangential wind component,

$$\frac{\partial}{\partial z}\left(K\frac{\partial u}{\partial z}\right)$$

b. lateral eddy diffusion of the tangential wind component,

$$\frac{\partial}{\partial r}\left[K_H\left(\frac{\partial u}{\partial r}+\frac{u}{r}\right)\right]$$

b. vertical eddy diffusion of sensible heat,

$$\frac{\partial}{\partial z}\left(K\frac{\partial \theta}{\partial z}\right)$$

d. lateral eddy diffusion of sensible heat,

$$K_H\left(\frac{\partial \theta}{\partial r^2}+\frac{1}{r}\frac{\partial \theta}{\partial r}\right)$$

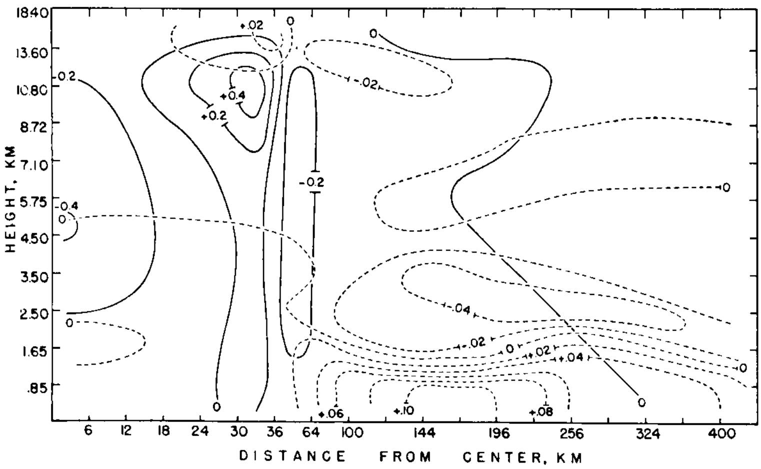

FIG. 8. The contributions to the vertical (cm sec^{-1}, full lines) and the radial (m sec^{-1}, dashed lines) velocity fields by vertical eddy diffusion of heat.

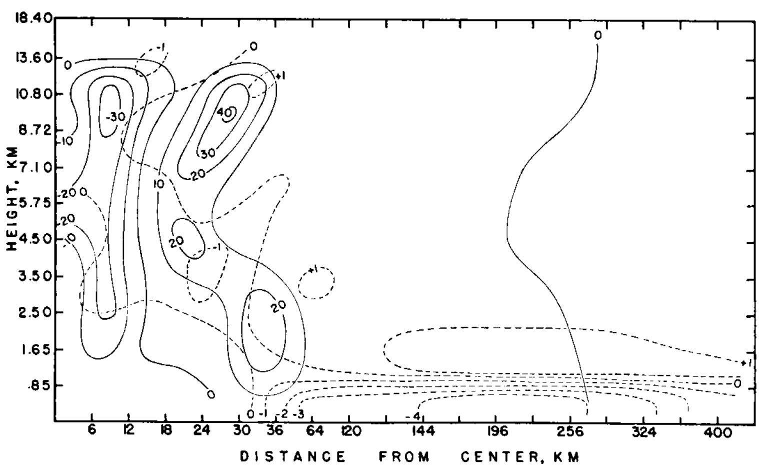

FIG. 9. The total contribution by vertical and lateral eddy diffusion processes of both tangential wind and heat to the vertical (cm sec^{-1}, full lines) and radial (m sec^{-1}, dashed lines) velocity fields.

e. heating by condensation,

$$\Gamma^* w$$

The separate contributions of each of these processes may be seen in Figs. 5 to 9.

Figs. 5 and 6 show that the strong ascending motions in the eye wall are contributed by both the vertical and lateral eddy diffusion in the tangential wind component. The former contributes to the low-level maximum while the latter, to the two maxima in the middle and the upper regions. The descending motions in the eye are primarily associated with the lateral diffusion of heat (Fig. 7) away from the warm core. The vertical eddy diffusion of heat (Fig. 8) contributes very little to the computed vertical circulation.

It may also be seen that the shallow radial inflow is mostly associated with vertical eddy exchange processes in the tangential wind component near the ground; this effect is similar to the observed in dishpan experiments. The same process also gives an outflow immediately above the low-level inflow. On the other hand, the lateral eddy exchange of the tangential velocity gives maximum outflow near the top

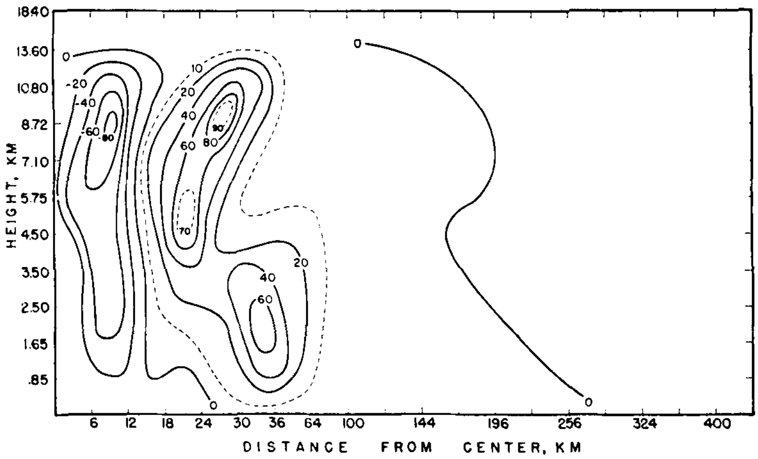

FIG. 10. The computed vertical velocity field (cm sec^{-1}) for the case which includes the effect of evaporational cooling.

and away from the region of maximum upward motions.

Fig. 9 shows the sum of all the processes indicated by items *a* to *d*. Comparing it with Fig. 3, one may see that the heating by condensation intensifies the upward motions in the eyewall by approximately twice that due to turbulent exchange processes alone. There appears to be very little effect of condensation heating in the eyewall on the computed downward motions in the eye.

It is often suggested that evaporative cooling is appreciable within the eye region. In order to obtain a crude estimate of the effect of this non-adiabatic cooling on the computed circulation, we integrated Eq. (6) on the assumption that descent occurs along the moist adiabatic instead of the dry adiabatic lapse rate. This is done by setting $\Gamma^* = L/\phi^* \, \partial q_m/\partial z$ for both positive and negative values of w. The computed vertical motion field (Fig. 10) shows intensification of the descending motions in the eye by approximately twice that for the case without cooling by evaporation (Fig. 3). The vertical motions outside the eye are relatively unaffected.

5. Discussion

The computed vertical and radial motions exhibit many of the important characteristics of a mature hurricane—downward motions in the central core (the eye), strong upward motions immediately surrounding the eye, a relatively shallow inflow in the lowest layers, and outflow aloft. It is interesting to note that a similar circulation has been obtained by KRISHNAMURTI (1961). His computations, which were based on a steady state, axially-symmetric model, used a slightly different tangential velocity distribution. A comparison between the two results reveals two main differences in the circulation patterns. First, the depth of his inflow layer is much larger compared with our results. Thus, at a radius of 150 km away from the center, his depth is almost an order of magnitude larger.

The second difference is concerned with the basic dynamics of the eye. In his model, descent in the eye is entirely associated with lateral mixing in the tangential wind. In our study, however, downward motion in the eye is controlled by the lateral mixing of potential temperature and, to a slight degree, of the tangential wind component. The eddy diffusion of heat away from the warm core and cooling by evaporation act effectively as a heat sink with respect to the larger-scale motions. In our formulation, this would imply descending motions just as a heat source would imply upward motions. The different implications concerning the processes which maintain the eye indicated by these two studies certainly require further scrutiny.

6. Summary and conclusions

The vertical and radial motions in a mature tropical cyclone have been calculated theoretically from prescribed tangential velocity and temperature distributions. The main assumptions introduced are those of axial symmetry, quasi-gradient wind balance, and hydrostatic equilibrium. The theoretical results have reproduced such features as the eye, the eyewall, the low-level radial inflow, and the high-level outflow. The results have shown also that the descending motions in the eye are associated mainly with the eddy diffusion of heat by lateral exchange processes from the warm core while the low-level indraft is associated with vertical exchange processes in the tangential wind field near the earth's surface. The mechanism of the eye circulation indicated by the results is a thermally-controlled process similar to that envisioned by ELIASSEN (1959). This is in contrast with that suggested by KUO (1959) and KRISHNAMURTI (1961) which is based on frictional drag by the strong ascending currents in the eyewall.

Acknowledgement

The author wishes to thank Professor Ronald Lavoie and Mr. Francis Ho for programming the computations and for their many helpful suggestions during the study. Thanks are also due to Mr. Lionel Medeiros for drafting the figures.

The research was supported by the National Science Foundation (Grant No. G14770).

REFERENCES

ELIASSEN, A., 1952: Slow thermally or frictionally controlled meridional circulations in a circular vortex. *Astrophysica Norvegica*, **5**, no. 2.

ELIASSEN, A., 1959: On the formation of fronts in the atmosphere. *The Rossby Memorial Volume*, Rockefeller Institute Press, N.Y.

LAVOIE, R. L., 1956: An evaluation of radar results from hurricane research flights of 1955. (Unpublished M.S. degree thesis, Florida State University, 26 pp.)

KRISHNAMURTI, T. N., 1961: On the vertical velocity field in a steady symmetric hurricane. *Tellus*, **13**, pp. 171–180.

KUO, H. L., 1959: Dynamics of convective vortices and eye formation. *The Rossby Memorial Volume*, Rockefeller Institute Press, N.Y.

PEDERSEN, K., 1961: *On the vertical circulation produced by release of latent heat in a static and quasi-geostrophic atmosphere*. Department of Meteorology, Univ. of Chicago, 12 pp.

RIEHL, H. and J. MALKUS, 1961: Some aspects of Hurricane Daisy, 1958. *Tellus*, **13**, pp. 181–213.